DOSE VERIFICATION OF 3D PRINTED MALE PELVIC PHANTOM FOR RADIOTHERAPY QUALITY ASSURANCE

PERAVEEN A/L M MANIAM

UNIVERSITI SAINS MALAYSIA

2024

DOSE VERIFICATION OF 3D PRINTED MALE PELVIC PHANTOM FOR RADIOTHERAPY QUALITY ASSURANCE

by

PERAVEEN A/L M MANIAM

Dissertation submitted in partial fulfilment
of the requirements for the degree of
Bachelor of Health Science (Honours) (Medical Radiation)

August 2024

ACKNOWLEDGEMENT

First and foremost, I would like to thank my parents for their constant love and encouragement. Their unwavering support and belief in me have been my greatest source of strength throughout my academic journey. Secondly, I am very grateful to my supervisor, Dr. Jayapramila A/P Jayamani for providing me with her guidance, patience and expertise throughout my research project. Her mentorship has challenged me to think critically and independently which greatly contributed to my personal and academic growth. Thirdly, I would like to extend my sincere gratitude to Kamaros Eliyati for permitting me to use the phantom she developed for her research study in my own research project.

Next, I would like to thank my field supervisor, Miss Arifah Nazirah Abdullah for her hands-on support during my data collection at the radiotherapy department of Hospital Universiti Sains Malaysia. Special thanks to the medical physicist in the department, En. Reduan Bin Abdullah, for also assisting me with data collection and for sharing valuable knowledge that supported my research. Additionally, I am also grateful to Madam Nor Shazleen Ab. Shukor for teaching me how to use equipment for thermoluminescence dosimetry.

Moreover, I would like to express my sincere appreciation to my colleagues especially Yuni Sara and Adriana Batrisyia who have supported me emotionally and practically, throughout this research project. Lastly, I would like to acknowledge all those who contributed to this work, directly or indirectly. Your support and encouragement have been incredibly meaningful to me.

TABLE OF CONTENTS

LIST OF TABLES

Page

LIST OF FIGURES

Page

LIST OF SYMBOLS

cGy	Centigray
cm	Centimeter
°	Degree
˚C	Degree Celsius
ρ	Density
d_{max}	Depth of maximum dose
$D_{x\%}$	Dose received by x% of GTV
g/cm^3	Gram per cubic meter
Gy	Gray
HU	Hounsfield unit
CF_i	Individual calibration factor
S_i	Individual sensitivity correction factor
kV	Kilovoltage
<	Less than
D_{max}	Maximum dose
$\bar{R}$	Mean reading of all TLDs
MV	Megavoltage
µC	Microcoulomb
µGy	Microgray
mm	Millimeter
MU	Monitor Unit
>	More than
nC	Nanocoulomb
%	Percentage
±	Plus-minus

R_i	Thermoluminescence reading of i-th detector
V_x	Volume receiving x Gy of radiation dose
$V_{x\%}$	Volume receiving x% of radiation dose

LIST OF ABBREVIATIONS

ABS	Acrylonitrile butadiene styrene
AAPM	American Association of Physicist in Medicine
AAA	Analytical Anisotropic Algorithm
CT	Computed tomography
JPNRO	Department of Nuclear medicine, Radiotherapy and Oncology
EBRT	External beam radiotherapy
FDM	Fused deposition modelling
HUSM	Hospital Universiti Sains Malaysia
IMRT	Intensity modulated radiotherapy
ICRP	International Commission on Radiological Protection
LINAC	Linear accelerator
MLC	Multi-leaf collimator
OSLD	Optically stimulated luminescent dosimeter
OAR	Organ at risk
PSQA	Patient-specific quality assurance
PMT	Photomultiplier tube
PET	Polyethylene terephthalate
PLA	Polylactic acid
PMMA	Polymethyl methacrylate
SSD	Source-to-surface distance
SD	Standard deviation
SABR	Stereotactic ablative radiotherapy
TG	Task group
TLD	Thermoluminescent dosimeter
3D-CRT	Three-dimensional conformal radiotherapy

3D	Three-dimesnioanl
TPS	Treatment planning system
2D	Two-dimensional
USM	Universiti Sains Malaysia
VMAT	Volumetric modulated arc therapy

LIST OF APPENDICES

PENGESAHAN DOS MENGGUNAKAN FANTOM PELVIS LELAKI CETAKAN 3D UNTUK JAMINAN KUALITI RADIOTERAPI

ABSTRAK

Kanser prostat adalah isu kesihatan yang serius di seluruh dunia dan rawatannya merangkumi teknik radioterapi maju yang memerlukan jaminan kualiti spesifik pesakit (PSQA) untuk keselamatan dan ketepatan rawatan. Fantom PSQA komersial adalah homogen dan tidak mimik interaksi foton di pelvis manusia. Oleh itu, sebuah fantom yang heterogen dan mimik pelvis lelaki telah dicipta menggunakan teknologi pencetakan tiga dimensi (3D). Dalam kajian ini, bahan fantom tersebut dicirikan oleh ketumpatan fizikal dan nombor tomografi berkomputer (CT) serta profilnya. Selain itu, pengesahan dos dilakukan menggunakan fantom dengan dosimeter pendarcahaya terma - 100 (TLD-100) dan kebuk pengionan. Keputusan menunjukkan bahawa fantom pelvis sepadan dengan kepadatan dengan perbezaan maksimum 0.22 g/cm^3 untuk prostat. Nombor CT pada 120 kV sepadan dengan nombor CT organ sebenar dengan perbezaan yang berkisar dari 12.30 HU hingga 189.77 HU. Profil CT pada 90 kV, 120 kV, dan 140 kV menunjukkan bar ralat standard yang kecil dan bertindih yang membuktikan keragaman yang tinggi dalam pencetakan 3D. Pengesahan dos menggunakan fentom pelvis lelaki 3D menunjukkan dalam pelan 3D-CRT bahawa pengiraan TPS bersetuju dalam ±5% dan ±2% untuk pengukuran TLD-100 dan kebuk pengioanan, masing - masing. Ujian Mann-Whitney U untuk 3D-CRT menunjukkan tiada perbezaan yang signifikan antara dos yang dikira TPS dan dos yang diukur dosimeter ($p > 0.05$). Dalam pelan VMAT, pengiraan TPS menunjukkan dos yang lebih rendah di GTV berbanding pengukuran oleh TLD-100

(deviasi: -14.1% hingga -17.1%) dan kebuk pengionan (deviasi: -4.8%), walaupun tiada perbezaan yang signifikan secara statistik ditemui oleh ujian Mann-Whitney U ($p > 0.05$). Kesimpulannya, pengiraan dos TPS dan pengukuran dosimeter menggunakan fentom pelvis lelaki cetakan 3D dalam pelan 3D-CRT menunjukkan persetujuan dalam had yang diterima, tetapi pengesahan lanjutan diperlukan untuk memastikan dosimetri yang tepat dalam pelan VMAT.

DOSE VERIFICATION OF 3D PRINTED MALE PELVIC PHANTOM FOR RADIOTHERAPY QUALITY ASSURANCE

ABSTRACT

Prostate cancer is a serious health concern worldwide, and its treatment includes advanced radiotherapy techniques that requires patient-specific quality assurance (PSQA) for safety and accuracy of the treatment. Commercially available PSQA phantoms are homogeneous and fail to mimic photon interactions in the pelvis. Therefore, a heterogeneous 3D printed male pelvic phantom was developed to replicate the male pelvis. In this study, the phantom material was characterized by its physical density and computed tomography (CT) numbers and profile. In addition, dose verification was conducted using the phantom with thermoluminescent dosimeter-100 (TLD-100) and ionisation chamber. The results show that the phantom matches the density of real human organs with a maximum difference of 0.22 g/cm^3 for prostate. The CT numbers measured at 120 kV well matched with the CT number of real organ with differences ranging from 12.30 HU to 189.77 HU. CT profiles at 90 kV, 120 kV, and 140 kV exhibited consistent gray values with small variation and overlapping standard error bars, indicating high uniformity in the 3D printing. Dose verification using the 3D printed male pelvic phantom revealed in 3D-CRT plans that TPS calculations agreed within ±5% and ±2% for TLD-100 and ionisation chamber measurements, respectively. The Mann-Whitney U test for 3D-CRT showed no significant differences between TPS calculated dose and the dosimeters measured dose ($p > 0.05$). In VMAT plans, the TPS calculations showed lower doses in the GTV compared to measurements by TLD-100 (deviations: -14.1% to -17.1%) and ionisation

chamber (deviation: -4.8%), despite no statistically significant difference found by the Mann-Whitney U test ($p > 0.05$). In conclusion, the dose calculations and measurements using the 3D printed male pelvic phantom in 3D-CRT plans demonstrated agreement within acceptable limits, but further verification is essential to ensure accurate dosimetry in VMAT plans.

CHAPTER 1

INTRODUCTION

1.1 Background of the Study

Prostate cancer stands as a substantial health concern worldwide. According to Global Cancer Observatory, prostate cancer ranks second in the world among male cancers, accounting for about 14.2% of all male cancer cases worldwide and ranked third among Malaysian males, accounting for approximately 9.5% of all male cancer cases in the country in 2022 (Ferlay *et al.*, 2024). In addressing the challenges of dealing with this disease, various treatment modalities such as prostatectomy, hormone therapy, chemotherapy, and radiotherapy offer hope for patients, with radiotherapy standing out for its effectiveness and minimal impact on quality of life (National Cancer Institute, 2024; Chancellor, 2023).

Radiotherapy, particularly external beam radiotherapy (EBRT) is a type of cancer treatment in which a machine called linear accelerator (LINAC) directs high-energy ionizing radiation from outside the body towards the tumour (National Cancer Institute, 2018). Advancement in radiotherapy over the past several years has led to the employment of dynamic radiotherapy techniques such as Intensity modulated radiotherapy (IMRT) and volumetric modulated arc therapy (VMAT) to treat prostate cancer (Posiewnik & Piotrowski, 2019). The use of these sophisticated techniques enables precise and accurate delivery a very high radiation dose to the target volume while minimizing damage to the organ at risks surrounding the target volume (Yadav al., 2021; Sun et al., 2022).

Nevertheless, the downside of advanced radiotherapy techniques lies in the heightened complexity of treatment plan or the need for increased radiation beam

modulation. This complexity arises from the combinations of numerous irregularly shaped and small beam segments, aimed at achieving higher dose conformity to target volume. The increased complexity in treatment planning may lead to reduction in the accuracy of the treatment delivery by the LINAC (Wall & Fontenot, 2021). Thus, ensuring the patient receives safe and accurate treatment necessitates the performance of patient specific quality assurance (PSQA) (Choi *et al.*, 2021)

The PSQA is a dosimetry measurement process that is performed to verify the treatment planning system (TPS) calculated dose and the deliverability of linear accelerator (LINAC) when advanced planning techniques such as IMRT and VMAT are applied for treating the patient (Giacometti *et al.*, 2021). The PSQA are often performed using radiotherapy quality assurance phantoms combined with dosimeters. The commercially available phantoms such as the ArcCheck and Octavius 4D phantoms have homogenous density which is equivalent to of water (ρ = 1 g/cm^3) (Tino *et al.*, 2019).

However, the human body, specifically pelvis, is inhomogeneous in nature, consist of bones and organs that have different densities. According to the International Commission on Radiological Protection (ICRP) Publication 110 (2009), the densities of the human bladder, prostate, rectum, and femoral heads are 1.04 g/cm^3, 1.03 g/cm^3, 1.04 g/cm^3 and 1.52 g/cm^3, respectively. A study by Yadav et al. (2023) demonstrated varying dose discrepancies in patient specific dosimetry due to tissue heterogeneity. The percentage difference between planned and measured doses ranges from 2.5% to 10.5% in heterogeneous phantoms compared to less than 3% in homogeneous phantoms. The study highlights the importance of using a phantom that closely mimics the actual human body in terms of density and design for patient specific dosimetry.

A three - dimensional (3D) printing is a modern technology that has become increasingly popular in a wide range of fields including in the field of medical physics (Tino *et al.*, 2019). It is a manufacturing process that creates physical objects by layer-by-layer method of printing. The advantages of 3D printing technology such as their diverse range of materials and customization capabilities has made it possible to create heterogenous phantoms for radiotherapy quality assurance (Kim *et al.*, 2017). Many researchers have successfully developed heterogenous phantoms through the utilization of 3D printing technology (Kamomae et al., 2017; Yea et al., 2017; Zhang et al., 2019; Choi et al., 2021; Giacometti et al., 2021; Yadav al., 2021). However, in order to ensure the developed phantom is a reliable tool for PSQA, a comprehensive validation process is essential. Therefore, the aim of this study is to verify the 6 MV photon interaction on the 3D printed male pelvic phantom.

1.2 Problem Statement

The rapid growth of technology in radiotherapy emphasizes the increasing importance of PSQA in delivering accurate and safe radiotherapy treatment for cancer patients (Han *et al.*, 2023). Commercial phantoms for PSQA in radiotherapy are homogenous because they are made of materials similar to water. For instance, ArcCHECK and Octavius phantoms is made of polymethyl methacrylate (PMMA) and polystyrene respectively. The homogenous commercial phantom doesn't fully mimic the male pelvis, which contains bones and organs of different densities. Therefore, it can't accurately represent how photons interact in the heterogeneous human pelvis, Additionally, the production of the commercially available phantom is expensive, which raises the price at which they are sold (Tino *et al.*, 2019).

The commercially available phantoms such as the ArcCHECK and Octavius phantoms are integrated phantoms in which the dosimeters are rigidly embedded within the phantom at fixed positions. This limits the flexibility in choosing measurement positions and geometries. Additionally, it also limits the choice of dosimeters. The integrated phantoms commonly employ diodes or ionisation chambers for dosimetry. Diodes are prone to radiation-induced changes that affects their response over time. They are also affected by energy and temperature fluctuations, as well as low-energy scatter. In other hand, ionisation chambers require larger measurement volume to produce usable signal-to-noise levels. Other dosimeters such as thermoluminescent dosimeter (TLD), optically stimulated luminescent dosimeter (OSLD) or radiochromic film may offer different measurement capabilities but are not compatible with the commercial phantoms.

The development of 3D printing technology offers a way to potentially overcome the drawbacks of commercially available phantoms by producing a customizable phantom that can be designed to resemble human tissue and employ various dosimeters at a reasonable cost (Tino *et al.*, 2019). However, since 3D printing involves layer-by-layer printing process there is chances for the phantom to have defects due to as inappropriate adhesion, poor solidification, shrinkage, and inadequate bond between filaments layers (Ali *et al.*, 2023). Besides, Cherpak and Chytyk-Praznik (2024) also stated that completely homogenous density is not achieved even with 100% infill setting when 3D-printing due to very small unavoidable gaps between printed layers (Robar, 2024). This necessitates, inspection of the developed phantom for any flaws within it. In addition, it is important to ascertain the fidelity of the phantom is accurately representing the male pelvic region in terms of radiological characteristics (Dewerd & Kissick, 2014).

Moreover, a thorough verification of dosimetry characteristics of the phantom is essential prior to its application in PSQA. Previous studies have highlighted the importance of validating a phantom by verification of dose using it (Kamomae et al., 2017; Giacometti et al., 2021; Yadav al., 2021). The comprehensive validation of the phantom will allow to address the aforementioned issues, ensuring the reliability and accuracy of the phantom for PSQA in radiotherapy. Thus, in this study dose verification is done using the developed 3D printed male pelvic phantom to evaluate the feasibility of its usage in radiotherapy dosimetry.

1.3 Research Questions

a) How the profile of the developed 3D – printed organs are affected under 90 kV, 120 kV and 140 kV CT scans?

b) What are the differences between the TPS calculated dose and measured dose (TLD and ionisation Chamber) in 6 MV photon beam?

1.4 Objective

1.4.1 General Objective

The main objective of this study is to verify the 6 MV dose interaction on the 3D printed male pelvic phantom for radiotherapy quality assurance.

1.4.2 Specific Objective

a) To analyze the profile of the developed 3D printed organs in 90 kV, 120 kV and 140 kV using CT.

b) To validate the 3D printed phantom using open field in 3D-CRT planning technique in 6 MV photon beam

c) To compare Eclipse TPS calculated dose with measured dose (TLD-100 and ionisation chamber) in VMAT planning technique.

1.5 Study Hypothesis

a) H_O: There are no significant differences in dose between the TPS calculation and dosimeters (TLD and ionisation chamber) measurements performed using the 3D printed male pelvic phantom in 6 MV photon beam.

b) H_A: There are significant differences in dose between TPS calculation and dosimeters (TLD and ionisation chamber) measurements performed using the 3D printed male pelvic phantom in 6 MV photon beam.

1.6 Significance of Study

In the field of radiotherapy, 3D printing technology is currently undergoing active exploration and innovation, owing to the advantages it has demonstrated in the field (Tino *et al.*, 2019). The validation of the phantom will allow to address and resolve any issues associated with the development of the phantom. Successful validation will create possibilities for the potential utilization of the phantom for PSQA in radiotherapy and is not limited for prostate cancer but also for other types of cancers in the male pelvic region such as bladder and rectal cancer.

Besides, the phantom has overcome the limitation of the commercial phantoms in terms of the heterogeneity and represents the actual characteristics of the male pelvis. Moreover, the developed the phantom employs various types of dosimeters compared to conventional phantom which employs limited types of dosimeters. With these advantages, a more accurate pre-treatment dosimetry process can be done,

ultimately leading to the delivery of more accurate dose to tumour while minimizing damage to healthy tissue, which is the primary goal of radiotherapy.

In addition, this study will provide valuable benefits for researchers in the field of medical physics. By contributing to the understanding of verification of 3D printed phantom, more discoveries can be made towards the application of 3D printing in the field of medical physics especially in radiotherapy. Apart from its scientific significance, the developed phantom demonstrates entrepreneurship applicability, providing prospects for commercialization to healthcare facilities that operates radiotherapy centre.

CHAPTER 2

LITERATURE REVIEW

2.1 Prostate Cancer

The prostate is an accessory sex gland found in all male mammals. In humans, the prostate has a doughnut shape and is approximately the size of a golf ball. It has dimensions of approximately 4 cm in width, 3 cm in height and 2 cm in depth. As shown in Figure 2.1, the gland envelopes the prostatic urethra and is located inferiorly to bladder and anteriorly to rectum. The function of prostate is to secrete a milky, slightly acidic fluid that constitutes one quarter of the semen volume and nourishes the sperm. The malignancy characterized by the abnormal proliferation of cells in the prostate gland is known as prostate cancer (Tortora & Derrickson, 2017).

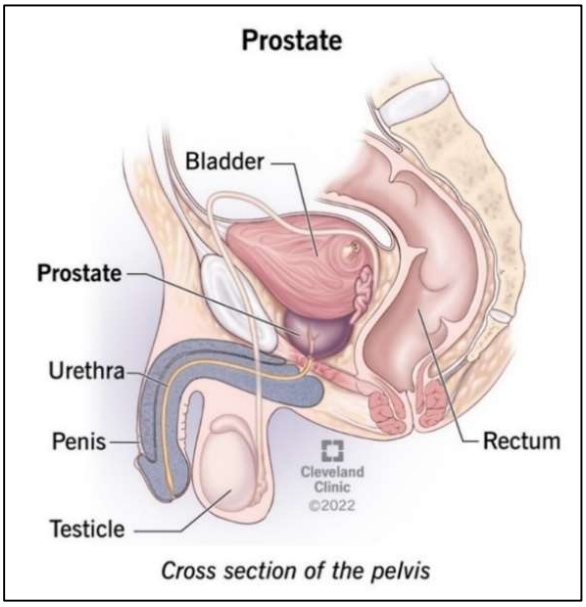

Figure 2.1: Cross section of the pelvis showing the anatomical position of the prostate gland in relation to the bladder, rectum, urethra, penis and testicle (Cleveland Clinic, 2023).

2.1.1 Prostate Cancer Statistics

Amidst the ongoing challenges of our modern world, prostate cancer persists as an important health issue, ranking as the second most diagnosed cancer after lung cancer and fifth leading cause of cancer mortality among men globally as depicted in Figure 2.2. In 2022 alone, it accounted for 1,467,854 new cases and 397,430 deaths. In Malaysia it ranks as the third most diagnosed cancer, accounting for 2360 cases and the fifth leading cause of death, with 1058 deaths in 2022. It is expected that the new case and deaths will increase by 62.7% and 68.3% respectively in Malaysia by the year 2035 (Ferlay *et al.*, 2024).

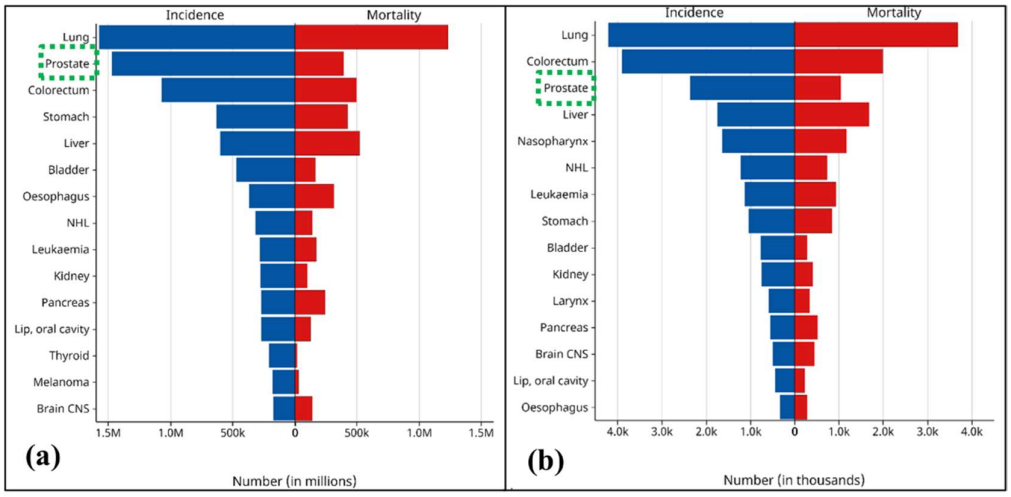

Figure 2.2: Incidence and Mortality among males in 2022 for top 15 cancer sites (a) globally and (b) in Malaysia (Ferlay *et al.*, 2024).

2.1.2 Prostate Cancer Symptoms and Diagnosis

According to the American Cancer Society (ACS) (2023), the causes of prostate cancer remain poorly defined, but there are several factors that can heighten the risk of developing the disease. These include older age, ethnicity, family history, obesity, smoking, dietary patterns. At an early stage, prostate cancer is often asymptomatic but may include urination symptoms such as bone pain due to

difficulties and blood in the urine or semen. Advanced prostate cancer can exhibit symptoms like erectile dysfunction, fatigue, and bone pains due to distant organ metastasis. However, these symptoms are general and necessitate further examination.

Prostate cancer is usually diagnosed through various methods. Initially, a digital rectal examination is performed to assess the prostate for abnormalities. Following this, a prostate-specific antigen (PSA) test that measures the PSA levels in blood. These tests don't necessarily confirm prostate cancer but may indicate benign enlargement or infection (Tortora & Derrickson, 2017). Further assessment often involves biopsy in which the prostate tissue samples are taken for microscopic analysis. Additionally, imaging modalities such as CT, magnetic resonance imaging and bone scan may be performed to evaluate the extent of cancer spread (ACS, 2023). Based on the diagnosis, the prostate cancer is staged into 4 stages as illustrated in Figure 2.3.

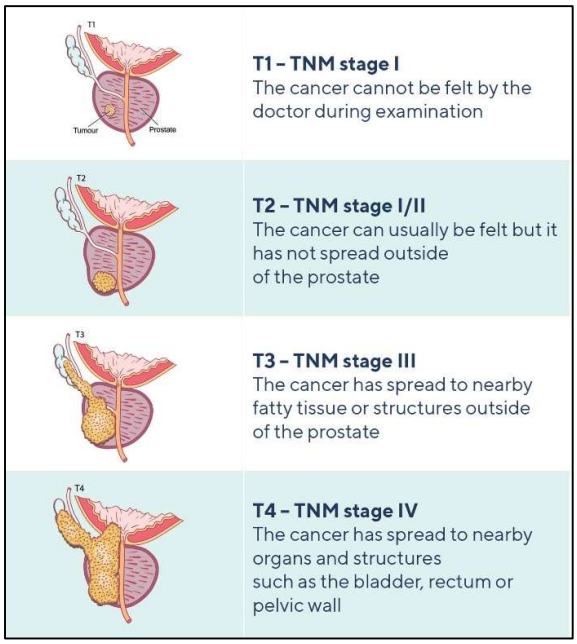

Figure 2.3: TNM staging for prostate cancer (Prostate Cancer Foundation of Australia, 2024).

2.1.3 Prostate Cancer Treatments

Once the diagnosis of prostate cancer is confirmed, the focus shifts to figuring out the best treatment for the patients according to individual patient's diagnosis and circumstances. The three common treatment options for prostate cancer are prostatectomy, hormonal therapy, and radiotherapy (Li *et al.*, 2021). Prostatectomy is an invasive procedure in which the prostate, surrounding tissue, seminal vesicle, and nearby tissues are removed. The main prostatectomy techniques include open radical prostatectomy, laparoscopic radical prostatectomy, robot-assisted laparoscopic radical prostatectomy, and transurethral resection of the prostate (National Cancer Institute, 2024).

Hormone therapy, also known as the androgen deprived therapy (ADT) is a treatment which involves removing or inhibiting the activity of androgens, mainly testosterone which are responsible for the growth of prostate cancer cells. This is achieved by the usage of drugs or orchiectomy to reduce the amount of testosterone produced in the body. Besides, radiotherapy stands as a radical treatment modality in which high-energy ionizing radiation such as x-rays or particle radiations is delivered to the prostate to kill the cancer cells. Further elaboration on this topic will ensue in the next section. In addition, active surveillance, chemotherapy, and immunotherapy are among the treatments used for prostate cancer (National Cancer Institute, 2024).

2.2 Radiotherapy for Prostate Cancer

Radiotherapy is an established modality in managing prostate cancer patients. The two types of radiotherapy used for prostate cancer are brachytherapy and EBRT. Brachytherapy involves the insertion of radioactive source right inside or close to the

tumour. Whereas in EBRT high energy radiation is delivered to the tumour from an external radiation source. The first reported use of EBRT for prostate cancer dates back to 1960s and by the early 1980s EBRT gained recognition as an acceptable treatment modality for prostate cancer. By the 1990s, clinical results were demonstrating that the results of radiotherapy are comparable to those achieved with radical prostatectomy (Greco & Zelefsky, 2000).

2.2.1 LINAC

In a LINAC as illustrated in Figure 2.4, electrons are produced by thermionic emission from electron gun. These electrons are then accelerated by a radiofrequency power generator and propelled along an along a linear path within an accelerating waveguide. The high energy electrons are then bent through at an appropriate angle (typically 90˚ or 270˚) by a bending magnet to strike the heavy metal x-ray target to produce high-energy x-ray photons for treating deep seated tumours. Alternatively, the high-energy electrons produced by the LINAC can be used without striking the x-ray target to treat superficial cancers. These radiation beams are then modulated to conform the shape and size of tumour using the multi-leaf collimator (MLC) in the LINAC head. Besides, the gantry of LINAC can be rotated to direct the radiation beam towards the tumour from various angles while the patient lies on the treatment couch (Gibbons, 2020).

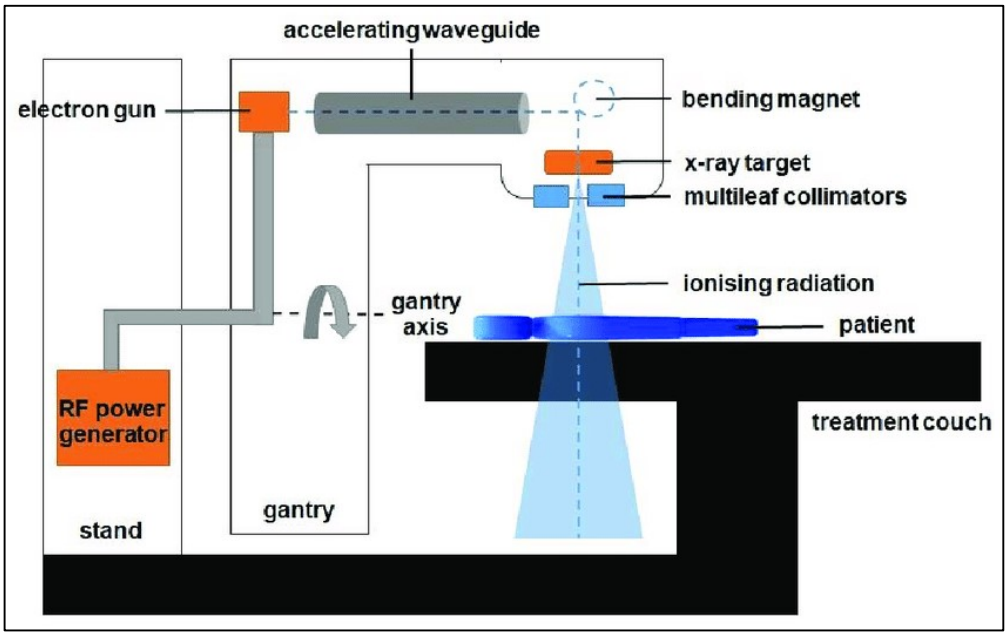

Figure 2.4: Schematic diagram of a LINAC and its components (Mohyedin *et al.*, 2022).

2.2.2 Conventional EBRT Technique

Over the past decades, advancements in computer technologies and machinery have improved the EBRT planning and delivery techniques. This advancement has introduced the 3D-CRT technique which utilizes volumetric images to create treatment plans, enhancing tumour localization and showing the healthy organs at risk (OARs) structures. In prostate 3D-CRT, multiples radiation beams are strategically placed at various angles, with the MLC conformed to the tumour volume as shown in Figure 2.5. This allows for improved dose conformity compared to the previous two-dimensional planning technique. However, 3D-CRT is now considered a conventional method as more sophisticated techniques have emerged over the years (Greco & Zelefsky, 2000).

2.2.3 Advanced EBRT Techniques

IMRT is and advanced form of 3D-CRT that uses inverse planning technique in which the treatment plans are created based on user-specified constraints for tumour volume and OARs, by using various computer-based optimization techniques. Same as in 3D-CRT, in IMRT multiple radiation beams are employed from various gantry angles. However, the intensity of each beam modulated by employing the MLC that act as a physical filter during the delivery of treatment. Thus, IMRT delivers a more conformal dose to tumour volume and reduced dose to OARs compared to 3D-CRT as shown in Figure 2.5 (Meyer, 2011).

There are two types of IMRT which are the step-and-shoot IMRT and sliding window IMRT. In step step-and-shoot IMRT each radiation beam is delivered using multiple segments created by the MLCs. The radiation dose is only delivered when the MLCs are stationary, and no dose is delivered when the MLC move to the next segment. In contrast, the sliding window IMRT modulates the beam intensity by continuously moving the MLC while the beam is on. The sliding window technique offers advantages over the step-and-shoot technique, including improved dose homogeneity to the tumour volume and reduced treatment time (Metcalfe, Kron & Hoban, 2007).

VMAT is an evolution of IMRT which incorporates an arc – based approach to deliver radiotherapy. In VMAT, radiation is delivered continuously as the machine gantry rotates around the patient. The continuous gantry rotation combined with the dynamic movement of MLC and dose rate variations enables the delivery of high conformal dose to the target volume in a shorter time compared to IMRT that employs limited number of gantry angles as shown in Figure 2.5. Besides, the number of segments per arc and the total number of arcs influences the degree of beam intensity

modulation in VMAT. However, publications have indicated that for less challenging case such as prostate cancer, a single arc is sufficient to provide a high-quality treatment plan (Meyer, 2011).

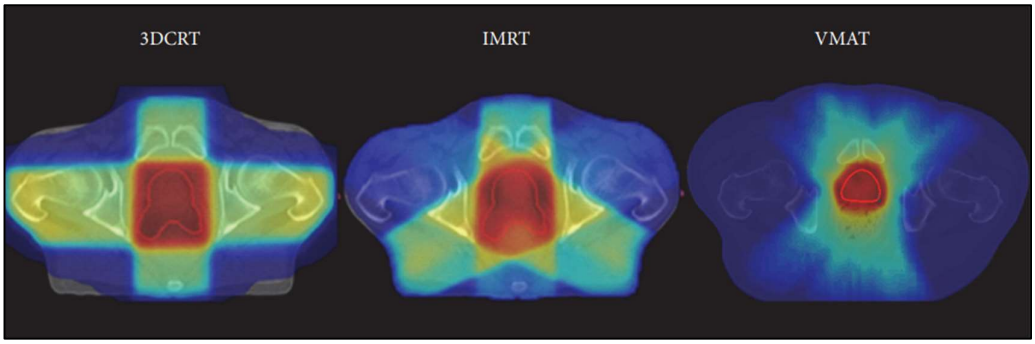

Figure 2.5: Dose distribution comparison between 3D-CRT, IMRT and VMAT (Vanneste *et al.*, 2016).

2.3 PSQA

PSQA is a critical process in radiotherapy to ensure the accuracy and safety of treatment process, particularly with advanced techniques like IMRT and VMAT. Although these advanced planning techniques offer significant advantages, such as delivering highly conformal doses to tumours with sharper dose gradients and reducing toxicity to OARs, they also involve complex and less intuitive planning and treatment delivery procedures that include intricate movements of MLC, gantry rotations, and dose rate variations (Meyer, 2011).

In addition to that, any errors occurring in the TPS, during the transfer of the plan from TPS to the delivery system, or in actual dose delivery by the LINAC can lead to undesirable treatment outcomes (Low *et al.*, 2018). Therefore, PSQA is performed to determine whether the LINAC accurately delivers the treatment plan as created in the TPS. This process involves using one or more dosimeters integrated with

a phantom and is conducted after the treatment plan is approved by the radiation oncologist, prior to the first treatment session of the patient (Miften *et al.*, 2018).

The first step in PSQA involves the transferring of the patient's treatment plan beam information to the CT image of a phantom using the copy-to-phantom feature in TPS, and the dose is recalculated by the TPS based on the phantom's geometry. Then, the plan is transferred to the delivery system, the phantom is irradiated, and the dosimeter measured dose is compared with the TPS calculated dose according to national or international guidelines such as the American Association of Physicists in Medicine Task Group 218 (AAPM TG 218) report. If the measurement falls within the tolerance, the treatment can proceed as planned (Metcalfe al., 2007; Miften et al., 2018).

2.4 Dosimeters Used in PSQA

A radiation dosimeter is defined as an instrument that is used to measure ionizing radiation directly or indirectly in terms of a specific quantity, such as exposure, kerma, absorbed dose or equivalent dose. From a physics perspective, a dosimeter used for radiotherapy should measure the ionizing radiation in terms of absorbed dose which is defined as energy absorbed per unit mass. Dosimeters can be categorized as absolute or relative. An absolute dosimeter generates signal from which the dose can be determined without calibration in a known radiation field, whereas a relative dosimeter requires calibration in a known radiation field to determine the dose (Podgorsak, 2005)

The AAPM TG 120 report provides a comprehensive overview of the dosimeters detailing their appropriate applications and limitations for the IMRT QA. In this report, the dosimeters are classified into point dosimeters, two-dimensional

(2D) dosimeters and 3D dosimeters. Point dosimeter measures the dose at specific points, and it includes ionisation chambers, diode detectors and TLDs. Whereas the 2D dosimeters can measure the dose distributions in a 2D plane and it includes film, detector arrays and computed radiography. Lastly, 3D dosimeters able to measure the dose distribution in 3D space and the main type of 3D dosimeters include polyacrylamide gels, Fricke gels and radiochromic plastics (Low *et al.*, 2011).

2.4.1 Ionisation chamber

Ionisation chamber is the most widely used dosimeter for dose measurement in radiotherapy. It can be used as absolute or relative dosimeter (Podgorsak, 2005). The advantage of ionisation chamber is it has excellent stability, linear response to absorbed dose, small directional dependence, beam quality response independence and traceability to a primary calibration standard (Low *et al.*, 2011). In PSQA, the cylindrical ionisation chamber as shown in Figure 2.6 is used. The ionisation chamber has a thimble wall that that encloses an air cavity which act as the sensitive volume. The chamber volume may vary from 0.007 cm^3 to 0.6 cm^3 (Miften *et al.*, 2018). The inner surface of thimble wall is coated with conducting material to form an electrode. In addition, the ionisation chamber has a central electrode that made of low atomic number material such as aluminium or graphite (Gibbons, 2020).

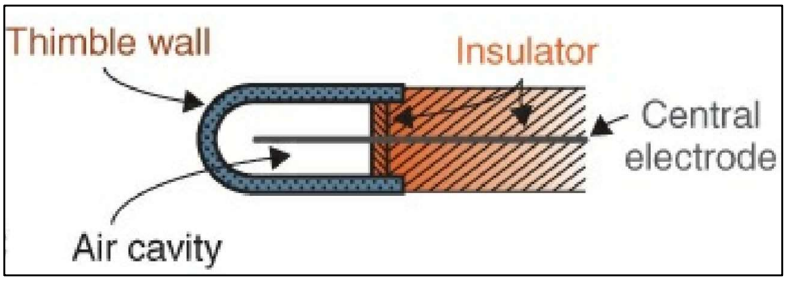

Figure 2.6: Schematic diagram of a cylindrical ionisation chamber (Gibbons, 2020).

When the ionisation chamber is exposed to ionizing radiation, interactions within the air cavity produces ion pairs. The ion pairs produced in the air cavity is collected by applying a suitable voltage between the two electrodes which results in a measurable charge. The charge is then measured by an electrometer which is connected to the ionisation chamber using a shielded cable (Gibbons, 2020). The requirements for the electrometer used are accuracy, linearity, stability, sensitivity, high impedance and low leakage (Low *et al.*, 2011).

2.4.2 TLD

TLDs are relative dosimeters that absorb and store the energy of ionizing radiation, which is then re-emitted as light upon heating. The emitted light is detected and correlated to the absorbed radiation dose (Mayles et al., 2007). TLDs have various applications in radiotherapy, including in vivo dosimetry for patients, personal monitoring, environmental monitoring, and verification of treatment techniques in different phantoms (Cherry & Duxbury, 2009). They are available in various forms such as microcubes, disk, powder, threadlike and chips as shown in Figure 2.7.

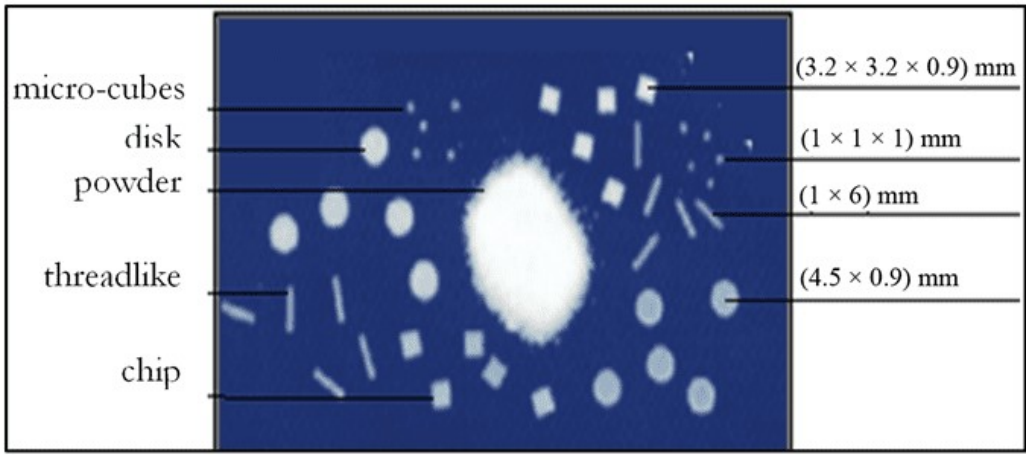

Figure 2.7: Various forms of TLD (Oncology Medical Physics, n.d.).

The most commonly used TLD in radiotherapy is lithium fluoride doped with magnesium and titanium (LiF:Mg,Ti), also known as TLD-100. This preference is due to its tissue equivalence (effective atomic number of 8.2, similar to 7.4 for tissue), low signal fading (5-10% per year), wide linear response range (10μGy – 10 Gy), high sensitivity for low-dose measurement, and small size (Liuzzi *et al.*, 2015). According to the AAPM TG 120, TLDs can be used for dose verification using radiotherapy phantoms when the geometry of the phantom does not allow for ion chamber measurements and when multiple simultaneous point measurements are required (Low *et al.*, 2011).

2.4.2(a) Principle of TLD

The principle of TLD involves using crystalline materials with impurities that create electron traps between the conduction and valence bands. At room temperature, electrons are in the valence band, and the conduction band is empty. When the material is exposed to ionizing radiation, the electrons are excited to the conduction band, and their prompt return to the valence band produces light (photon) emission, known as fluorescence. Some electrons get trapped in metastable states. When these electrons gain sufficient energy, they are excited to conduction band and fall back to the valence band, resulting in the emission of light, known as phosphorescence. Heating the material speeds up this process, and the phenomenon is known as thermoluminescence, as shown in Figure 2.8.

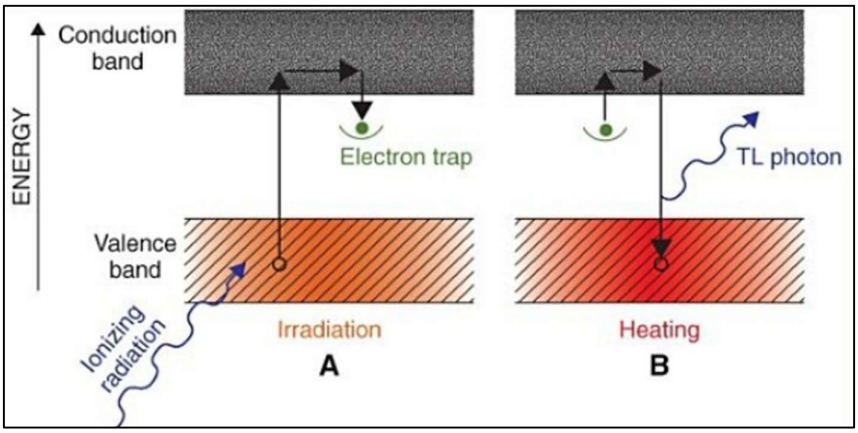

Figure 2.8: Energy-level diagram illustrating thermoluminescence process (Gibbons, 2020).

2.4.2(b) TLD Reader system

The TLD reader system as shown in Figure 2.9, measures radiation doses by heating TLD on a planchet, releasing trapped electrons. These electrons emit light, which is collected and guided by a light guide, then detected by a photomultiplier tube (PMT). The signal integrator amplifies and direct the light emission to an integrator or converts and feeds it to a scaler, producing a glow curve. The data is then stored and processed by a PC and its associated software (Mayles et al., 2007).

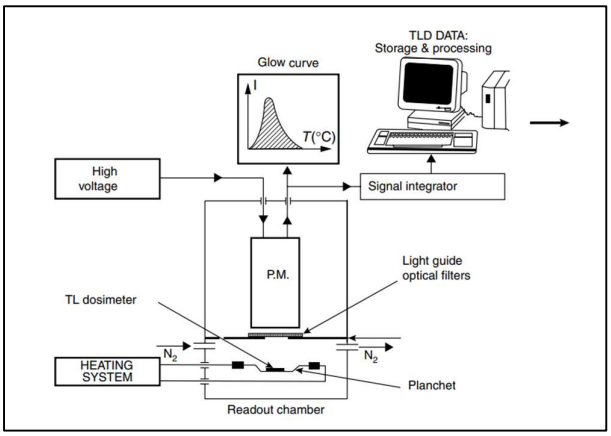

Figure 2.9: Components of planchet heating TLD reader system (Mayles et al., 2007).

2.5 Phantoms

According to Mosby's Medical Dictionary, a phantom is defined as a mass of material similar to human tissue used to investigate the effect of radiation beam on human beings. Phantoms are crucial in radiotherapy for simulating the conditions of specific procedures to measure dose at certain points of interests. Exposing real human for the purpose of dose measurement in impractical and dangerous and inserting dosimeters inside a human body is even more so. Therefore, performing measurements on phantoms that represent human is safer and more practical as these test objects can receive repeated amounts of radiation dose (Dewerd & Kissick, 2014).

2.5.1 Commercially Available PSQA Phantoms

One of the commercially available PSQA phantom is the ArcCHECK phantom (Sun Nuclear Corporation, Melbourne, USA) as shown in Figure 2.10. This phantom is made of water-equivalent phantom material, which is PMMA, with a density of 1.15 g/cm^3. The phantom has a simple cylindrical geometry with a diameter and length of 27 cm and 43 cm, respectively. It has a central cavity that can fit various inserts such as a homogenous PMMA core, dosimetric core that can hold ion chamber and more. Besides, the phantom is integrated with an array of 21 cm equipped with 1386 diode detectors in a helical geometry with 10 mm offset, allowing for 3D dose measurement (Aristophanous *et al.*, 2016). The SNC patient software provided by the manufacturer allows to compare the ArcCHECK measured dose with TPS planned dose using distance to agreement, gamma, and gradient compensation (Sun Nuclear Corporation, n.d.).

Figure 2.10: ArcCHECK phantom (Sun Nuclear Corporation, n.d.).

Another commercially available PSQA phantom is the Octavius 4D phantom (PTW Freiburg, Freiburg, Germany) as shown in Figure 2.11. The Octavius 4D phantom is constructed from polystyrene material with a density of 1.05 g/cm^3, closely matching the density of water. It has a cylindrical shape with diameter of 32 cm and a length of 34.3 cm. The phantom includes three detector arrays with varying numbers and types of ionisation chambers tailored for advanced IMRT/VMAT quality assurance and stereotactic radiosurgery applications. It also includes a semi-cylindrical air cavity in its lower region to correct the non-water equivalence of the detector arrays (Douama *et al.*, 2021). Additionally, it incorporates an inclinometer that enables synchronous rotation of phantom with gantry, ensuring the beam always hits the detector array perpendicularly. The data analysis is supported by the PTW Verisoft software which offers advanced tools for evaluating gamma index analysis and dose distributions (PTW Dosimetry, n.d.).

Figure 2.11: Octavius 4D phantom with its detector array (PTW Dosimetry, n.d.).

2.6 3D Printing Technology

3D printing, also known as additive manufacturing, has transformed many industries since its introduction in the 1980s. This manufacturing technology enables the creation of a physical object by building up layers of materials based on digital models. Over the past few decades, 3D printing has evolved from a niche technology used primarily for prototyping in industrial settings to a more accessible and versatile tool that is utilized across various fields including healthcare. Its widespread adoption is attributed to its advantages such as cost-effectiveness, a wide range of materials, and the ability to customize products with desired geometric features (Robar, 2024).

In the healthcare field, common application of 3D printing includes surgical planning, biocompatibility assessment, 3D printed prostheses, hospital quality management, treatment machine quality assurance, procedure risk assessment and more (Robar, 2024). According to a report published by Acumen Research and Consulting (2023), the global 3D Printing in medical applications market size reached USD 2.8 Billion in 2022 and is expected to reach USD 11 Billion by 2032, with a compound annual growth rate of 16.6% from 2023 to 2032, as shown in Figure 2.12.

The rapid growth trajectory highlights the role of 3D printing in healthcare, emphasizing its impact and potential for further advancements in the field.

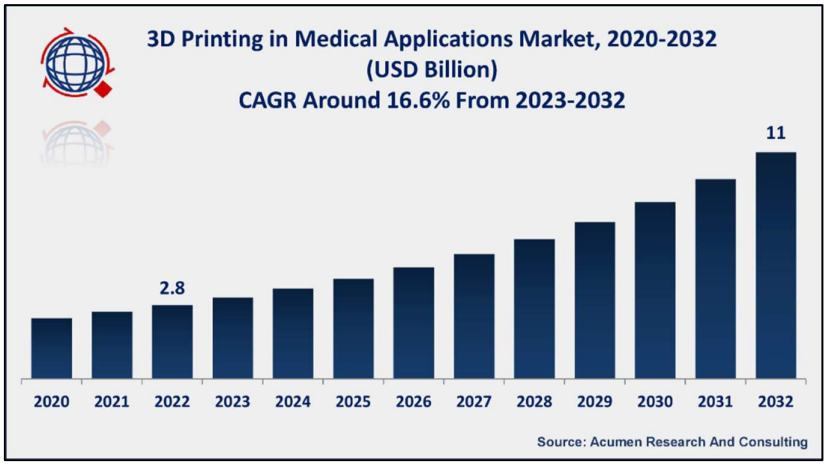

Figure 2.12: Projected growth in the market value of 3D printing technologies used in medical applications from 2020 to 2032 (Acumen Research and Consulting, 2023).

2.6.1 3D Printing Technology in Radiotherapy

In recent years, 3D printing has made significant impact in the field of medical physics, especially in radiotherapy. A review conducted by Tino et al. (2019) examined 10,266 publications up to July 2018, revealing several key findings. Among these, imaging phantoms accounted for the highest percentage of publications (38%), followed by dosimetry phantoms (24%). Furthermore, 3D printing has been employed in various other applications within radiotherapy, including bolus fabrication (13%), immobilizers (8%), compensators (4%), brachytherapy moulds (10%), and electron beam cutouts (3%). Figure 2.13 provides an illustration of these findings, showcasing the trend in the application of 3D printing technology in radiotherapy.